· Article ·
doi: 10.13679/j.advps.2014.1.00032

Advances in Polar Science
March 2014 Vol. 25 No. 1: 32-37

GPS-based regional ionospheric models and their suitability in Antarctica

AN Jiachun[1*], WANG Zemin[1] & NING Xinguo[1,2]

[1] Chinese Antarctic Center of Surveying and Mapping, Wuhan University, Wuhan 430079, China;
[2] Changchun Institute of Surveying and Mapping, Changchun 130021, China

Received 22 December 2013; accepted 19 February 2014

Abstract There are a number of ionospheric models available for research and application, such as the polynomial model, generalized trigonometric series function model, low degree spherical harmonic function model, adjusted spherical harmonic function model, and spherical cap harmonic function analysis. Using observations from more than 40 continuously operating stations across Antarctica in 2010, five models are compared with regard to their precision and applicability to polar regions. The results show that all the models perform well in Antarctica with 0.1 TECU of residual mean value and 2 TECU of root mean square error.

Keywords **GPS, ionospheric TEC, regional model, Antarctica**

Citation: An J C, Wang Z M, Ning X G. GPS-based regional ionospheric models and their suitability in Antarctica. Adv Polar Sci, 2014, 25: 32-37, doi: 10.13679/j.advps.2014.1.00032

1 Introduction

The polar upper atmosphere is one of the most active parts of Earth's atmosphere and near-Earth space, and study of the polar upper atmosphere will contribute to the overall understanding of the interactions between the solar wind, magnetosphere, ionosphere, and the upper and lower atmosphere[1]. As an important part of the polar upper atmosphere, the polar ionosphere has a significant role in monitoring, modeling, and forecasting services. GPS technology has the advantages of low cost, high precision, and wide coverage, and it is suitable for polar ionospheric research. GPS-based ionospheric Total Electron Content (TEC) modeling can be used to study ionospheric temporal variations[2-3], and ionospheric corrections in GPS signals[4]. A regional ionospheric model, which is more adaptable in certain areas, can be established using a number of GPS observation stations and comparison with the Klobuchar[4], IRI[5], Bent[6] or other global ionospheric models. Commonly, empirical ionospheric models contain a polynomial model (POLY for short)[7], e.g., the generalized trigonometric series function model (GTSF)[8], low spherical harmonic function model (LSH)[9], adjusted spherical harmonic function model (ASHF)[10], and spherical cap harmonic analysis (SCHA)[11]. In this paper, five models were achieved using data from more than 40 GPS stations across Antarctica in 2010 and their applicability to Antarctica was analyzed.

2 Regional ionospheric models

2.1 POLY

The POLY has a simple structure and takes into account ionospheric changes related to latitude and sun angle. This model is used widely in regional ionospheric modeling analysis because it can obtain better results than other models over a certain period and within a certain range. The model is based on the difference of sun angle and latitude difference between the ionospheric pierce point and the regional center,

* Corresponding author (email: jcan@whu.edu.cn)

and its expression is as follows[7]:

$$VTEC = \sum_{i=0}^{n}\sum_{k=0}^{m} E_{ik}(\varphi - \varphi_0)^i (S - S_0)^k \tag{1}$$

where E_{ik} are the unknown model coefficients, φ and S are the geographic latitude and sun angle at the ionospheric pierce point, respectively, and φ_0 and S_0 the geographic latitude and sun angle at the regional center, respectively.

2.2 GTSF

Within only a few hours, the POLY exhibits better fitting accuracy, and therefore Georgiadiou[8] proposed using a trigonometric series model to build a regional ionospheric model, which further improved the simulation capabilities of local daily ionospheric variations. Based on a trigonometric series, Yuan and Ou[9] presented a generalized trigonometric series with variable parameters in geomagnetic coordinates, as follows:

$$\begin{aligned} VTEC = {} & A_1 + \sum_{i=1}^{N_2}\left\{A_{i+1}\phi_m^i\right\} + \sum_{i=1}^{N_3}\left\{A_{i+N_2}h^i\right\} \\ & + \sum_{i=1,j=1}^{N_iN_j}\left\{A_{i+N_2+N_3}\phi_m^i h^j\right\} + \\ & \sum_{i=1}^{N_4}\left\{A_{2i+N_2+N_3+N_i+N_j-1}\cos(ih)\right. \\ & \left. + A_{2i+N_2+N_3+N_i+N_j}\sin(ih)\right\} \end{aligned} \tag{2}$$

where A_i are the generalized trigonometric series function model coefficients, φ_m is the geomagnetic latitude at IPP, and h represents variables related to local time. $h=2\pi(t-14)/T$, T = 24 h, where t is the local time at IPP in units of hours. $\varphi_m = \varphi + 0.064\cos(\lambda - 1.617)$, where φ and λ are the geographical latitude and longitude, respectively, in units of radians.

2.3 LSH

Schaer[10] analyzed the characteristics of a spherical harmonic function, simulated the regional and global ionosphere using the spherical harmonic function, and found it more accurate in global ionospheric model construction. Therefore, the spherical harmonic function has been used widely in global ionospheric models. A global spherical harmonic model with 15 × 15 order coefficients has been released by CODE. In global modeling, the zero-order term is the global ionosphere average TEC values. In regional modeling, although the spherical harmonic coefficients do not have orthogonality, a lower-order spherical harmonic function model can still be used to study the ionospheric region. The function model is as follows:

$$VTEC = \sum_{i=0}^{n}\sum_{k=0}^{m}(A_i^k \cos k\lambda' + B_i^k \sin k\lambda')P_i^k(\cos\varphi_m) \tag{3}$$

where λ' is the longitudinal difference between the pierce point and sun direct spot, $P_i^k(\cos\varphi_m)$ is the Legendre function, and A_i^k and B_i^k are unknown model coefficients.

2.4 ASHF

The orthogonality of the spherical harmonic function is derived from expansion on the sphere, but it is lost within a certain area. Through coordinate conversion, the projection can be changed from region to globe[11]. First, a spherical cap coordinate system is constructed, in which the new pole is the regional center, and the longitude line passing through the new pole and the geographic South Pole is taken as the initial meridian. Then, the original coordinates are transformed to a new coordinate system. The pole coordinates of the spherical cap coordinate system are (λ_0, φ_0) and the corresponding pierce point coordinates are (λ, φ); therefore, the new coordinates of the pierce point in the spherical cap coordinate system are (λ_c, φ_c). As the selected area is Antarctica, the center position is (0°E, 90°S), which means that $\varphi_c = -\varphi$ and $\lambda_c = \lambda$. Assuming the half-angle of the spherical cap is θ_{max}, the co-latitude of the pierce point in the spherical cap coordinate system is θ_c and its range is [0, θ_{max}], i.e., $\theta_c = \pi/2 - \varphi_c$. The longitude of the pierce point remains the same and the latitude is projected onto an assumed sphere with a certain proportion according to the half-angle of the spherical cap. Thus, the new coordinates are as follows:

$$\begin{cases} \varphi' = \dfrac{\pi}{2} - \theta', \theta' = \dfrac{\pi}{\theta_{\max}}\theta_c \\ \lambda' = \lambda_c \end{cases} \tag{4}$$

With this conversion, the pierce point coordinates are projected from the region to the assumed sphere, which meets the requirements for the fitting variables of the spherical harmonic function. The converted coordinates are introduced into formula (3) and the unknown coefficients calculated.

2.5 SCHA

As the basis functions of the spherical harmonics are no longer orthogonal in the local area, the spherical cap harmonic function is introduced. The basis functions of the spherical cap harmonics are orthogonal in the spherical region, and the zero-order term of the spherical cap harmonic coefficients indicate the average ionospheric TEC within the local area. The construction of the spherical cap coordinate system is the same as in section 2.4, but the main difference between SCHA, LSH, and ASHF is that the integer-order Legendre function is replaced by the non-integer-order Legendre function. The function model is as follows[12]:

$$\begin{aligned} VTEC = {} & \sum_{k=0}^{K_{\max}}\sum_{m=0}^{M}(\tilde{C}_{km}\cos m\lambda_c + \tilde{S}_{km}\sin m\lambda_c) \\ & \tilde{P}_{n_k(m),m}(\cos\theta) \end{aligned} \tag{5}$$

where $\tilde{C}_{km}$ and $\tilde{S}_{km}$ are fully regularized spherical harmonic coefficients; $\tilde{P}_{n_k(m),m}(\cos\theta)$ represents fully regularized non-integer-order Legendre functions.

3 Data processing

Three sources of GPS data were accessed. These included eight tracking stations in Antarctica built by the IGS (International GNSS Service[13]) and tracking stations in Antarctica built by POLENET (The Polar Earth Observing Network[14]). POLENET aims to collect GPS and seismic data, using an automatic remote data acquisition system built in Antarctica and Greenland, to study glacier change within the context of global warming. Although the layout of the stations in Antarctica is inland, by virtue of automatic mode, the distribution is mainly in western Antarctica. The third source comprises three tracking stations in Antarctica built by CACSM (the Chinese Antarctic Center of Surveying and Mapping): the Great Wall Station, Zhongshan Station, and Kunlun Station[15]. In particular, the data of Zhongshan and Kunlun stations provide an important supplement in eastern Antarctica. Figure 1 shows the distribution of the stations.

Because various problems occur in data collection, resulting in inaccurate data quality and mistaken formats, data pre-processing is necessary. The quality of IGS data is best, but POLENET and CACSM data have some problems. Therefore, TEQC[16], which is pre-processing software for GPS data, is used to verify the quality and output the data in a standard format. Then, highly accurate STEC (Slant TEC) is obtained with geometry-free linear combination using dual-frequency GPS pseudorange and phase measurements. The data-sampling rate is 30 s and the elevation is 10 degrees. The thin-shell or single-layer approach is used with a height of 370 km. VTEC (Vertical TEC) is obtained from STEC using the mapping function of 1/cos(z). All station data are calculated together to achieve the modeling. The model parameters and hardware delay are solved together[17]: every 2 h for one period, 12 periods a day, and the hardware delay is fixed daily. Generally, the satellite and receiver hardware delay are regarded as stable over 1 day[18]. To ensure smoothness between periods, some constraints are added[17]. To compare the effects of each model, nine parameters are chosen for the polynomial model, low sphere function model, improved sphere harmonic function model, and spherical cap harmonic function model, and the order and degree are two for the generalized trigonometric series: $N_2 = 0$, $N_i = N_j = 1$, $N_3 = 2$, $N_4 = 6$.

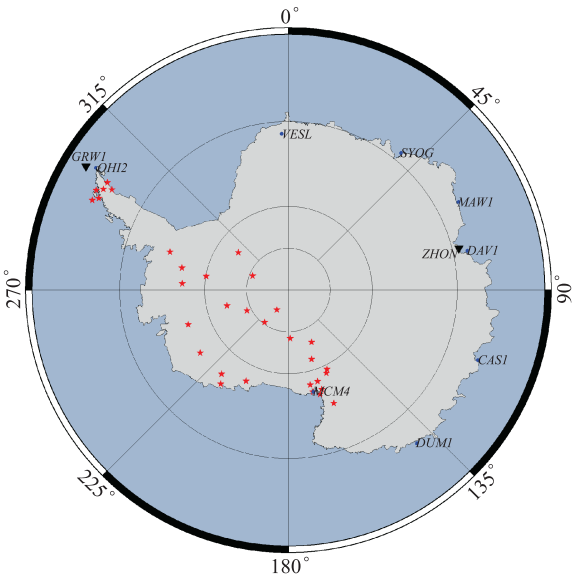

Figure 1 Distribution of the stations in Antarctica (● IGS stations, ★ POLENET, ▼ Chinese Antarctic stations)

4 Results and discussion

The five models are achieved using all the GPS data. After obtaining the model coefficients, inversed VTEC values at the pierce points are calculated. By comparing the inversed VTEC and measured VTEC, statistics are used to assess the precision, such as the daily residual mean (red dot-dash lines) as well as the daily RMS (solid green lines) in Figures 2–6. The horizontal axis is the day of the year, the left vertical axis is the residual mean, the right vertical axis is the root mean square error, and the unit is TECU.

Daily statistics of each model, such as the residual mean and root mean square, are listed in Table 1.

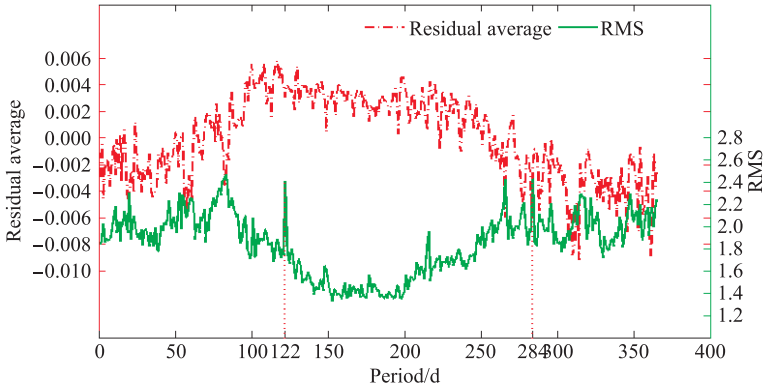

Figure 2 The statistics of POLY.

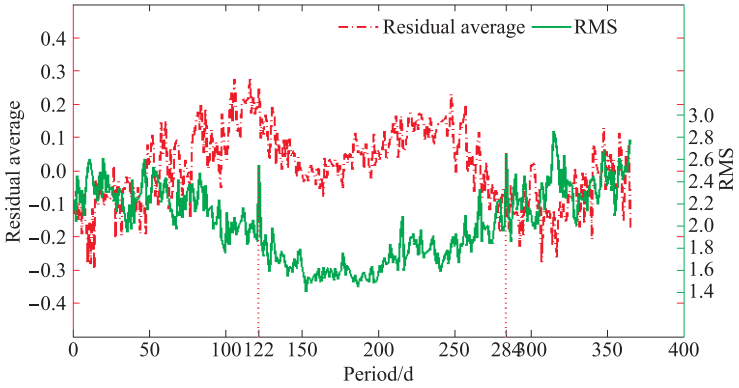

Figure 3 The statistics of GTSF.

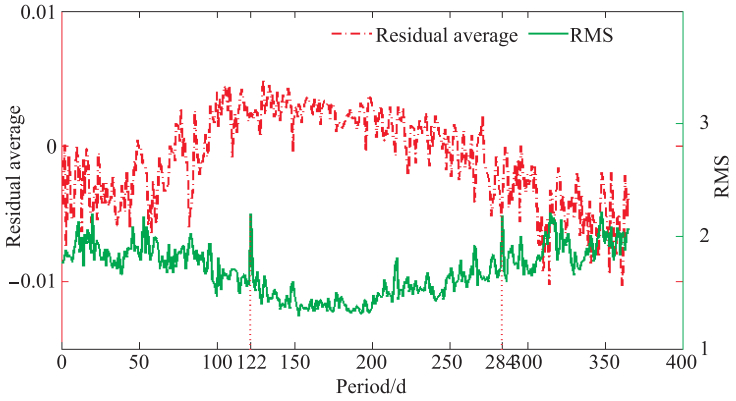

Figure 4 The statistics of LSH.

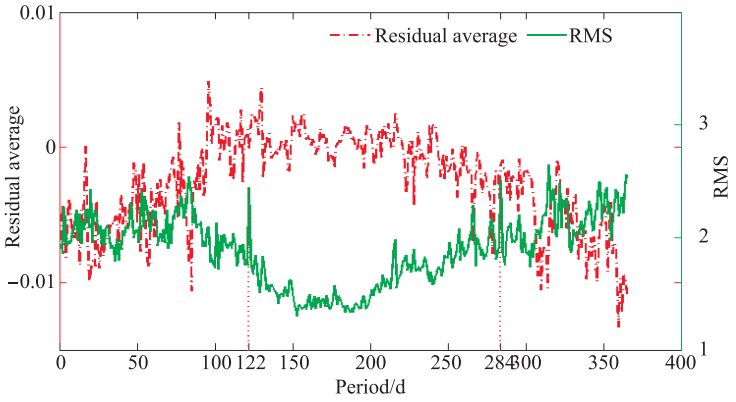

Figure 5 The statistics of ASHF.

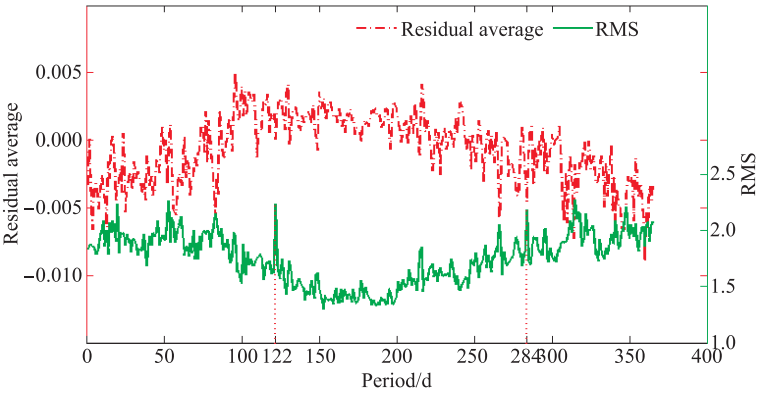

Figure 6 The statistics of SCHA.

Table 1 Annual residual average and RMS of all models

	POLY	GTSF	LSH	ASHF	SCHA
Residual average (10^{-4} TECU)	−0.85	78	−9.64	26	−7.5
Residual RMS (TECU)	1.84	2.02	1.69	1.89	1.74

The following discussion is based on the analysis above.

Figures 2 through 6 show that the changes in precision of the five models over 1 year are similar. The daily residual mean is substantially non-biased and very small, i.e., close to zero, and the root mean square error is less than 2 TECU. Especially for the polynomial model, low spherical harmonic function model, improved spherical harmonics function model, and spherical cap harmonic function model, the changes are very consistent, relatively speaking; whereas for the generalized trigonometric series function model, the values of the daily residual mean and RMS are larger. This is because the better daily fitting characteristics of this model are not fully reflected because of the time-sharing process of the models used for better comparison. During the winter in polar regions, the fitting effects of ionospheric models are better, e.g., the residual means are closer to 0 and the root mean square error falls to 1.5 TECU, because polar ionospheric activity is low in winter and the TEC value is small. In Antarctica, the ionospheric daily mean is only 1 TECU during winter, which is very small compared with that in low latitude regions, and thus the higher fitting precision not only illustrates the applicability of the models, it also has a certain relationship with polar ionospheric characteristics.

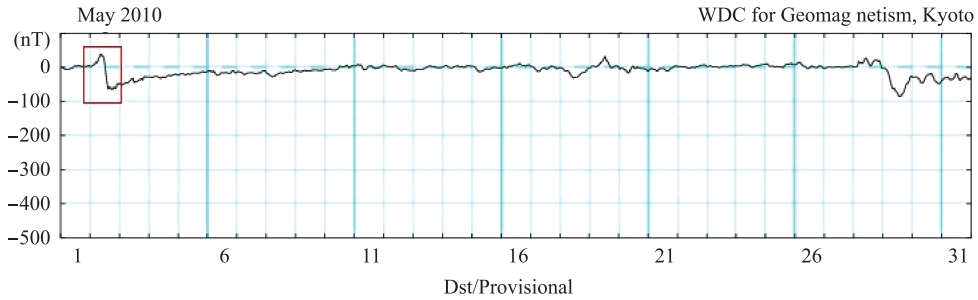

Figure 7 Magnetic Dst in May, 2010[18].

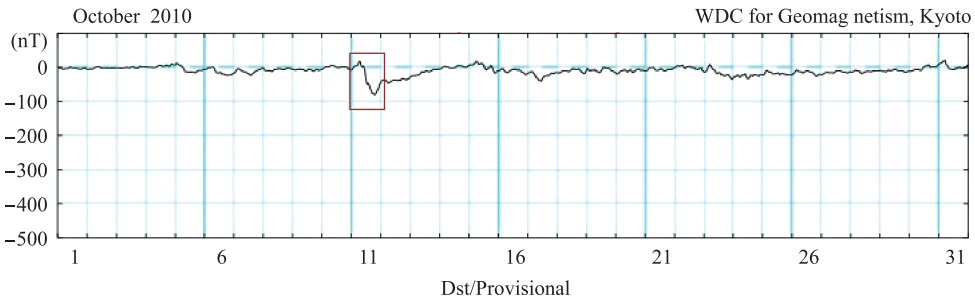

Figure 8 Magnetic Dst in October, 2010[18].

In addition to the apparent trend features, the five figures also show that on days 122 and 284 (corresponding to May 2 and October 11) the RMS exhibited major changes in magnitude; its value significantly exceeds the values of other periods. According to geomagnetic data of 2010 from the Japanese Global Geomagnetic Data Center[19], as shown in Figures 7 and 8, the Dst on those two days reached up to −66 and −80 nT, respectively, which indicates moderate geomagnetic storms ($-100 < \mathrm{Dst} \leqslant -50$ defines moderate geomagnetic storm). For all five ionospheric models, the RMS values displayed a similar transition within a certain time. Geomagnetic storms disturb the ionosphere and reduce the accuracy of GPS signals, which results in an increase of model-fitting errors.

5 Conclusions

In this paper, more than 40 GPS tracking stations in Antarctica are used to compare five empirical regional ionospheric models. The fitting accuracy of each model can reach 0.1 TECU for daily residual mean and 2 TECU for RMS error, which indicates good fitting effects. During periods of low ionospheric activity such as winter, the model accuracy is better, and compared with the mid-latitudes, the TEC in high latitudes is lower. During geomagnetic storms, the model-fitting effect declines rapidly. For a more detailed comparison of the models and more thorough analysis of the ionosphere, data with longer temporal scale and stations with more uniform spatial distribution are needed. Furthermore, the ionospheric data characteristics under both different seasons and states of geomagnetic activity must be considered further.

Acknowledgements This study was supported by the National Natural Science Foundation of China (Grant nos. 41174029, 41204028, 41231064), the Open Research Fund of Key Laboratory for Polar Science of SOA (Grant no. KP201201), the Chinese Polar Environment Comprehensive Investigation and Assessment Programs, the Science and Technology Project of NASMG (Grant name Polar Geomatics Technology Test). Data were issued by the Data-sharing Platform of Polar Science (http://www.chinare.org.cn) maintained by Polar Research Institute of China (PRIC) and Chinese National Arctic & Antarctic Data Center (CN-NADC).

References

1 Liu R Y, Yang H G. Progress in the polar upper atmospheric physics research in China. Chin J Pol Res, 2011, 23(2): 55-71.
2 Zhang Q H, Zhang B C, Lockwood M, et al. Direct observations of the evolution of polar cap ionization patches. Science, 2013, 339(6127): 1597-1600.
3 An J C, Wang Z M, E D C, et al. Ionospheric behavior and its effect on positioning during the solar eclipse of 22 July 2009. Chinese J Geophys, 2010, 53(10): 2291-2299.
4 Klobuchar J A. Ionospheric time-delay algorithm for single-frequency GPS users. IEEE Trans Aerospace Electron Syst, 1987, 23(3): 325-331.
5 Jee G, Schunk R W, Scherliess L. Comparison of IRI-2001 with TOPEX TEC measurements. J Atmos Solar-Terr Phy, 2005, 67(4): 365-380.
6 Ho C M, Wilson B D, Mannucci A J, et al. A comparative study of ionospheric total electron content measurements using global ionospheric maps of GPS, TOPEX radar, and the Bent model. Radio Sci, 1997, 32(4): 1499-1512.
7 Liu J B, Wang Z M, Zhang H P, et al. Comparison and consistency research of regional ionospheric TEC models based on GPS measurements. Geom Inform Sci Wuhan Univ, 2008, 33(5): 479-483.
8 Georgiadiou Y. Modeling the ionosphere for an active control network of GPS stations. Delft Geodetic Computing Centre, Delft, 1994.
9 Yuan Y B, Ou J K. A generalized trigonometric series function model for determining ionospheric delay. Prog Nat Sci, 2004, 14(11): 1010-1014.
10 Schaer S. Mapping and predicting the Earth's ionosphere using the Global Positioning System. Ph. D Dissertation, Bern, Switzerland: University of Bern, 1999.
11 Li Z S. GNSS/Compass ionospheric delay correction and TEC monitoring theory and method research. Ph. D thesis, Hubei: Institute of Geodesy and Geophysics, Chinese Academy of Sciences, 2012.
12 Liu J B, Chen R Z, Wang Z M, et al. Spherical cap harmonic model for mapping and predicting regional TEC. GPS Solutions, 2011, 15(2): 109-119.
13 International GNSS Service. http://igscb.jpl.nasa.gov/
14 POLENET. http://polenet.org/
15 An J C, Ai S T, Wang Z M. Monitoring and distribution system about TEC of polar ionosphere. Chinese J Polar Res, 2010, 22(4): 423-430.
16 TEQC−The Toolkit for GPS/GLONASS/Galileo/SBAS/Beidou/QZSS Data. http://facility.unavco.org/software/teqc/
17 Zhang H P, Ping J S, Zhu W Y, et al. Brief review of the ionospheric delay models. Prog Astron, 2006, 24(1): 16-26.
18 Sardon E, Rius A, Zarraoa N. Estimation of the transmitter and receiver differential biases and the ionospheric total electron content from Global Positioning System observations. Radio Sci, 1994, 29(3): 577-586.
19 World Data Center for Geomagnetism, Kyoto. http://wdc.kugi.kyoto-u.ac.jp/index.html